Nickel and Palladium Complexes of New Pyridine-Phosphine Ligands and Their Use in Ethene Oligomerization

Jitte Flapper,[†,‡] Huub Kooijman,[⊥] Martin Lutz,[⊥] Anthony L. Spek,[⊥] Piet W. N. M. van Leeuwen,[†] Cornelis J. Elsevier,[†] and Paul C. J. Kamer*[,†,§]

van 't Hoff Institute for Molecular Sciences, University of Amsterdam, Nieuwe Achtergracht 166, 1018WV Amsterdam, The Netherlands, Dutch Polymer Institute, PO Box 902, 5600 AX Eindhoven, The Netherlands, Bijvoet Center for Biomolecular Research, Crystal and Structural Chemistry, Faculty of Science, Utrecht University, Padualaan 8, 3584 CH Utrecht, The Netherlands, and School of Chemistry, University of St. Andrews, St. Andrews, Fife, Scotland KY16 9ST, U.K.

Received January 16, 2009

New pyridine-phosphine ligands of general structure 2-[2-(diarylphosphino)ethyl]pyridine were developed. The phosphorus substituents in these bidentates are 2-tolyl, 2-anisyl, and mesityl. The ligands could be conveniently synthesized in good yields. The nickel dichloride complexes of the ligands are paramagnetic. The metal centers have a distorted tetrahedral geometry, as was evident from the crystal structures and the magnetic moments in solution. The neutral methylpalladium chloride and the cationic methylpalladium complexes have a distorted square-planar geometry around the metal center. For the complexes of two of the ligands, an anagostic C−H···Pd interaction of a ligand-proton with the palladium atom was observed in the crystal structures and in solution. These interactions probably were related to hindered inversion of the six-membered metallocycle, which was observed in VT-NMR measurements. The complexes of the mesityl-substituted ligand show neither hindered inversion of the metal chelate ring nor a sign of Pd···H interactions. The nickel complexes form active catalysts for the oligomerization of ethene after MAO activation. The bulky 2-tolyl and mesityl groups suppress isomerization of the growing chain, reflected in a high 1-butene selectivity. For the complex made from the ligand with the most bulky (mesityl) substituents, this selectivity was 90%. The anisyl substituents induced a different catalytic behavior of the corresponding nickel complex. Selectivity for 1-butene was lower, but the productivity was higher, with a turnover frequency of 65×10^3 (mol C_2H_4)·(mol Ni·h)$^{-1}$. The cationic palladium complexes showed a very low activity in ethene oligomerization. Butenes were the major product, but significant amounts of higher olefins were formed as well.

Introduction

The oligomerization of ethene is an important industrial reaction, and megatons of α-olefins are produced yearly in this way. Depending on the chain length of the alkene, they are used for the production of various products. The most important ones are linear low-density polyethylene (LLDPE) (C4−C10), poly-α-olefins (C4, C10), plasticizers (C6−C10), lubricants (C8−C10), lube oil additives (C12−C18), and surfactants (C12−C20).[1,2]

In order to understand better the behavior of oligomerization catalysts and possibly improve their performance, much research is still devoted to the formation of olefins from ethene.[2,3] Among many transition metal complexes, nickel and—to a lesser extent—palladium complexes of P,N ligands (bidentate ligands with a phosphorus and a nitrogen donor atom) have been studied in this reaction. The development and application of P,N ligands is a significant field of homogeneous catalysis, and this ligand type has proven its value in many reactions.[4,5] We were particularly interested in pyridine-phosphine ligands. The chemistry of this class of ligand has been reviewed[4] and has been studied in nickel- and palladium-catalyzed ethene oligomerization.[2,6−10]

* To whom correspondence should be addressed. E-mail: pcjk@st-andrews.ac.uk. Fax: +44-(0)1334463808. Tel: +44-(0)1334-467285.
† University of Amsterdam.
‡ Dutch Polymer Institute.
⊥ Utrecht University.
§ University of St. Andrews.

(1) (a) Skupinska, J. *Chem. Rev.* **1991**, *91*, 613–648. (b) Al-Jarallah, A. M.; Anabtawi, J. A.; Siddiqui, M. A. B.; Aitani, A. M.; Al-Sa'doun, A. W. *Catal. Today* **1992**, *14*, 1–124. (c) Vogt, D. Oligomerization of ethylene to higher linear α-olefins. In *Applied Homogeneous Catalysis with Organometallic Compounds*; Cornils, B., Herrmann, W. A., Eds.; 1996; Vol. 1, pp 245−258.

(2) Speiser, F.; Braunstein, P.; Saussine, L. *Acc. Chem. Res.* **2005**, *38*, 784–793.

(3) (a) Hessen, B. *J. Mol. Catal. A: Chem.* **2004**, *213*, 129–135. (b) Dixon, J. T.; Green, M. J.; Hess, F. M.; Morgan, D. H. *J. Organomet. Chem.* **2004**, *689*, 3641–3668. (c) Wass, D. F. *Dalton Trans.* **2007**, 816–819. (d) Bianchini, C.; Giambastiani, G.; Rios, I. G.; Mantovani, G.; Meli, A.; Segarra, A. M. *Coord. Chem. Rev.* **2006**, *250*, 1391–1418. (e) Kuhn, P.; Semeril, D.; Matt, D.; Chetcuti, M. J.; Lutz, P. *Dalton Trans.* **2007**, 515–528. (f) Janiak, C. *Coord. Chem. Rev.* **2006**, *250*, 66–94. (g) Heinicke, J.; Peulecke, N.; Koehler, M.; He, M.; Keim, W. *J. Organomet. Chem.* **2005**, *690*, 2449–2457.

(4) (a) Chelucci, G.; Orru, G.; Pinna, G. A. *Tetrahedron* **2003**, *59*, 9471–9515. (b) Espinet, P.; Soulantica, K. *Coord. Chem. Rev.* **1999**, *195*, 499–556. (c) Newkome, G. R. *Chem. Rev.* **1993**, *93*, 2067–2089.

(5) (a) Braunstein, P. *J. Organomet. Chem.* **2004**, *689*, 3953–3967. (b) Braunstein, P.; Naud, F. *Angew. Chem., Int. Ed.* **2001**, *40*, 680–699. (c) Guiry, P. J.; Saunders, C. P. *Adv. Synth. Catal.* **2004**, *346*, 497–537. (d) Helmchen, G.; Pfaltz, A. *Acc. Chem. Res.* **2000**, *33*, 336–345. (e) Pfaltz, A.; Drury, W. J. *Proc. Natl. Acad. Sci. U.S.A.* **2004**, *101*, 5723–5726.

(6) (a) Bluhm, M. E.; Folli, C.; Walter, O.; Doring, M. *J. Mol. Catal. A: Chem.* **2005**, *229*, 177–181. (b) Bonnet, M. C.; Dahan, F.; Ecke, A.; Keim, W.; Schulz, R. P.; Tkatchenko, I. *J. Chem. Soc., Chem. Commun.* **1994**, 615–616. (c) Kermagoret, A.; Braunstein, P. *Organometallics* **2008**, *27*, 88–99. (d) Speiser, F.; Braunstein, P.; Saussine, L. *Organometallics* **2004**, *23*, 2625–2632. (e) Speiser, F.; Braunstein, P.; Saussine, L. *Organometallics* **2004**, *23*, 2633–2640.

10.1021/om900038u CCC: $40.75
Publication on Web 04/28/2009

Scheme 1. Synthesis of Ligands 1

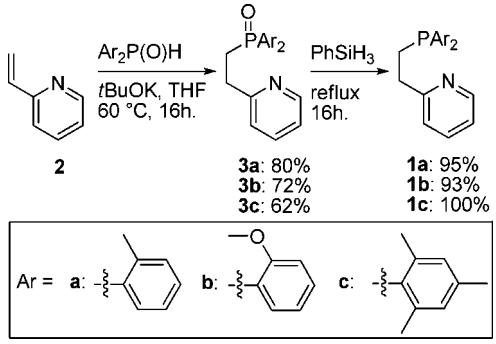

Scheme 2. Synthesis of Nickel Complexes 4

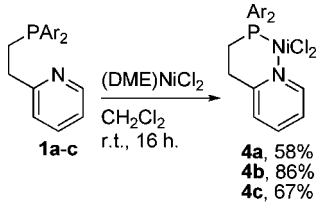

In this article, we present the development and study of pyridine-phosphine ligands (**1**) and their neutral nickel (**4**), neutral palladium (**5**), and cationic palladium (**6**) complexes. Complexes **4** (with MAO activation) and **6** were also evaluated for their potential as ethene oligomerization catalysts.

Results and Discussion

In this study we used P,N ligands **1a**−**c**, with a pyridine and a diarylphosphine donor group, connected by a 1,2-ethanediyl bridge. They differ in the aryl groups at the phosphine, which are 2-tolyl, 2-anisyl, and mesityl for **a**, **b**, and **c**, respectively.

Ligand Synthesis. The ligands were synthesized in two steps as depicted in Scheme 1. Base-catalyzed hydrophosphination of 2-vinylpyridine (**2**) with diarylphosphine oxides gave 2-[2-(diarylphosphinoyl)ethyl]pyridine compounds **3** in moderate to good yields. The secondary phosphine oxides used in this reaction can conveniently be prepared by reaction of aryllithium or Grignard reagents with diethylphosphite.[11,12] In the second step, phosphine oxides **3** were reduced using phenylsilane, and the 2-[2-(diarylphosphino)ethyl]pyridine ligands **1** were obtained in excellent yields. In the solid state, they are stable in air. In solution under aerobic conditions, they are slowly oxidized to phosphine oxides **3**.

Synthesis and Characterization of Nickel Complexes. The nickel dichloride complexes **4** were obtained from reaction of the ligands with (DME)$NiCl_2$ [DME = 1,2-dimethoxyethane]; see Scheme 2. After the reaction, the products were filtered through a pad of Celite to remove any unreacted (DME)$NiCl_2$. The solids obtained after evaporation of the solvent were washed with ether to remove any remaining free ligand, and this yielded the complexes **4** in pure form. All complexes exhibit a characteristic purple color in CH_2Cl_2 solution; in the solid state **4a** and **4c** are purple as well, while **4b** is a brown solid.

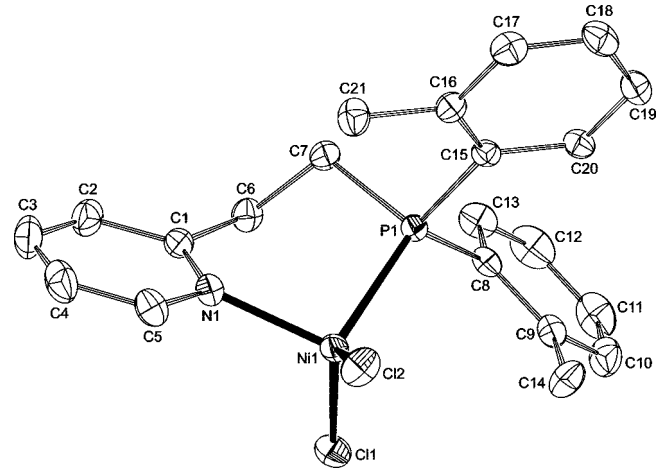

Figure 1. Displacement ellipsoid plot of **4a** in the crystal, drawn at the 50% probability level. Hydrogen atoms are omitted for clarity.

Table 1. Selected Angles (deg) and Bond Lengths (Å) in Complex 4a

P1−Ni1−N1	96.90(4)	Ni1−N1−C1	123.50(11)
P1−Ni1−Cl1	103.407(17)	N1−C1−C6	118.14(14)
P1−Ni1−Cl2	113.147(18)	C1−C6−C7	112.00(14)
N1−Ni1−Cl1	104.18(4)	C6−C7−P1	110.53(11)
N1−Ni1−Cl2	104.63(4)	C7−P1−Ni1	103.50(5)
Cl1−Ni1−Cl2	129.513(19)		
Ni1−P1	2.3036(4)	N1−C1	1.358(2)
Ni1−N1	2.0121(14)	P1−C7	1.8349(16)
Ni1−Cl1	2.2261(5)	C6−C7	1.549(2)
Ni1−Cl2	2.2151(5)	C1−C6	1.509(2)

The nickel complexes are paramagnetic, as evidenced by their magnetic moments in CD_2Cl_2 solution of 3.85 (**4a**), 3.30 (**4b**), and 3.30 μ_B (**4c**). These values are indicative of a distorted tetrahedral geometry of the nickel.[13] Using high-resolution mass spectrometry, the $[(ligand)NiCl]^+$ ion was observed for all complexes. Ionization of the complexes is accomplished by proton addition, which is immediately followed by loss of HCl, and this results in the formation of the observed ion. Elemental analyses for the nickel complexes were in agreement with the proposed structures. Compounds **4** were EPR-silent, as can be expected for this type of complexes.[14] In addition to the above-mentioned characterization, we performed single-crystal X-ray structure determinations on complexes **4a** and **4c**.

The X-ray crystal structure of complex **4a** is shown in Figure 1, and selected bond angles and distances are presented in Table 1. In agreement with the magnetic moment in solution, the nickel has a distorted tetrahedral geometry. As a result of the small bite angle of the ligand and the steric repulsion of the chlorides, the P−Ni−N angle is somewhat smaller than the ideal value of 109°, while the Cl−Ni−Cl angle is larger. The other angles around nickel are less distorted from tetrahedral. The other angles and the bond distances are in the normal range and do not require specification. The structure is similar to the related nickel dichloride complex **7** (see Chart 1).[9]

The X-ray crystal structure of **4c** is shown in Figure 2, and selected bond distances and angles are presented in Table 2.

(7) Chen, H.-P.; Liu, Y.-H.; Peng, S.-M.; Liu, S.-T. *Organometallics* **2003**, *22*, 4893–4899.
(8) Muller, G.; Klinga, M.; Osswald, P.; Leskela, M.; Rieger, B. *Z. Naturforsch., B: Chem. Sci.* **2002**, *57*, 803–809.
(9) Flapper, J.; Kooijman, H.; Lutz, M.; Spek, A. L.; Van Leeuwen, P. W. N. M.; Elsevier, C. J.; Kamer, P. C. J. *Organometallics* **2009**, *28*, 1180–1192.
(10) Flapper, J.; Van Leeuwen, P. W. N. M.; Elsevier, C. J.; Kamer, P. C. J. *Organometallics* **2009**, http://dx.doi.org/10.1021/om9000378.
(11) Busacca, C. A.; Lorenz, J. C.; Grinberg, N.; Haddad, N.; Hrapchak, M.; Latli, B.; Lee, H.; Sabila, P.; Saha, A.; Sarvestani, M.; Shen, S.; Varsolona, R.; Wei, X.; Senanayake, C. H. *Org. Lett.* **2005**, *7*, 4277–4280.
(12) Wife, R. L.; Van Oort, A. B.; Van Doorn, J. A.; Van Leeuwen, P. W. N. M. *Synthesis* **1983**, 71–73.
(13) Hayter, R. G.; Humiec, F. S. *Inorg. Chem.* **1965**, *4*, 1701–1706.
(14) Desrochers, P. J.; Telser, J.; Zvyagin, S. A.; Ozarowski, A.; Krzystek, J.; Vicic, D. A. *Inorg. Chem.* **2006**, *45*, 8930–8941.

Chart 1

7

Just as in **4a**, the metal has a distorted tetrahedral geometry, and this is in agreement with the paramagnetic nature of the complex in solution. The structure is similar to that of **4a**, although the P−Ni−N and Cl−Ni−Cl bonds are less distorted from perfect tetrahedral.

Synthesis and Characterization of Neutral Palladium Complexes. The methylpalladium chloride complexes **5** were obtained by reaction of the ligands with (COD)Pd(CH_3)Cl [COD = 1,5-cyclooctadiene]; see Scheme 3. Precipitation of the product with diethyl ether separated the metal complexes from free COD, and the pure complexes **5** were obtained in high yields.

The products were characterized by NMR, mass spectrometry, elemental analyses, and, for **5a** and **5b**, single-crystal X-ray structure determination. On the basis of the larger *trans* influence of the phosphorus compared to the nitrogen, it is expected that the methyl coordinates *cis* with respect to the phosphine. This coordination mode was indeed observed, as shown by the small $^3J_{P-H}$ coupling constant (3 to 4.5 Hz) between the phosphorus nucleus and the palladium-methyl protons. These solution phase observations are in agreement with the solid state structures of **5a** and **5b** obtained by single-crystal X-ray structure determinations; see below.

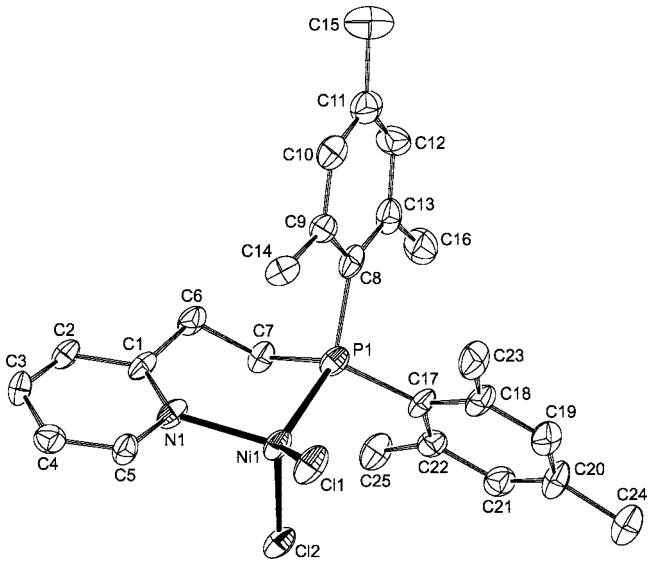

Figure 2. Displacement ellipsoid plot of **4c** in the crystal, drawn at the 50% probability level. Hydrogen atoms are omitted for clarity.

Table 2. Selected Angles (deg) and Bond Lengths (Å) in Complex 4c

P1−Ni1−N1	98.83(16)	Ni1−N1−C1	130.0(5)
P1−Ni1−Cl1	124.71(8)	N1−C1−C6	120.8(5)
P1−Ni1−Cl2	96.89(7)	C1−C6−C7	119.0(5)
N1−Ni1−Cl1	115.67(16)	C6−C7−P1	109.4(5)
N1−Ni1−Cl2	98.55(16)	C7−P1−Ni1	97.9(2)
Cl1−Ni1−Cl2	117.39(7)		
Ni1−P1	2.305(2)	N1−C1	1.361(7)
Ni1−N1	1.999(5)	P1−C7	1.837(6)
Ni1−Cl1	2.2158(18)	C6−C7	1.531(9)
Ni1−Cl2	2.244(2)	C1−C6	1.517(9)

Scheme 3. Synthesis of Neutral Palladium Complexes 5

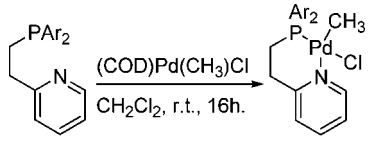

1a-c

5a: 88%
5b: 91%
5c: 81%

For complex **5c**, only sharp peaks were observed in the NMR spectra at ambient temperature. In the room-temperature ^{1}H and ^{13}C NMR spectra (recorded in $CDCl_3$) of **5a** and **5b**, on the contrary, broad peaks were observed. This is caused by hindered inversion of the six-membered palladium chelate ring, making the interconversion slow on the NMR time scale. When the proton spectra were recorded at −50 °C, all peaks appeared sharp. As a consequence of the slow ring inversion at this temperature, several nuclei became inequivalent. Especially notable is the large chemical shift difference for the *ortho*-aryl protons. The two signals for these protons are observed at 8.84 and 6.76 ppm (**5a**) and 8.66 and 6.55 ppm (**5b**). This can be explained by an anagostic interaction of one of these protons with the palladium atom.[15,16] This is also shown by relatively short Pd···H distances in the crystal structures of the complexes (see below). At 60 °C, the inversion of the chelate ring was fast on the NMR time scale, and as a consequence, only sharp peaks were visible in the NMR spectra. The aryl groups and the protons at each methylene were equivalent. The aromatic region of the variable-temperature ^{1}H NMR spectra for **5a** is shown in Figure 3. The spectra of the methylene region of **5a** and the aromatic and methylene regions of **5b** are given in the Supporting Information.

We have recently reported on the palladium complexes **8**−**10** (see Chart 2), which are related to complexes **5**.[9] Complex **10** also exhibited broad signals in room-temperature NMR spectra as a consequence of slow inversion of the metallocycle. In the crystal structure and NMR spectra, a Pd···H interaction was observed as well. Complexes **8** and **9** did not exhibit hindered inversion of the palladium chelate ring, nor did they show indications of short Pd···H distances. As the slow ring inversion is only observed for complexes that have an anagostic interaction of a proton with the axial position of the palladium, we believe this could explain these phenomena. The interaction of a proton with the axial position of the palladium atom could have a stabilizing effect, resulting in the observed hindered ring inversion.

We obtained the single-crystal X-ray crystal structure of complex **5a**. The structure is shown in Figure 4, and selected bond lengths and angles are given in Table 3. The complex is in a "boat" conformation and has a square-planar surrounded metal center. The methyl group is coordinated *cis* with respect to the phosphorus atom, which is in accordance with the NMR studies (see above). The bond angles around palladium show that the complex is only slightly distorted from perfect square planar. The most notable feature of the structure is the relatively

(15) Brookhart, M.; Green, M. L. H.; Parkin, G. *Proc. Natl. Acad. Sci. U.S.A.* **2007**, *104*, 6908–6914.

(16) For recent examples of palladium complexes showing anagostic (sometimes called preagostic) interactions, see: (a) Doherty, M. D.; Trudeau, S.; White, P. S.; Morken, J. P.; Brookhart, M. *Organometallics* **2007**, *26*, 1261–1269. (b) Han, Y.; Huynh, H. V.; Koh, L. L. *J. Organomet. Chem.* **2007**, *692*, 3606–3613. (c) Han, Y.; Huynh, H. V.; Tan, G. K. *Organometallics* **2007**, *26*, 6447–6452. (d) Trudeau, S.; Morken, J. P. *Tetrahedron* **2006**, *62*, 11470–11476. (e) Wurtz, S.; Glorius, F. *Acc. Chem. Res.* **2008**, *41*, 1523–1533. (f) Yen, S. K.; Koh, L. L.; Huynh, H. V.; Hor, T. S. A. *J. Organomet. Chem.* **2009**, *694*, 332–338.

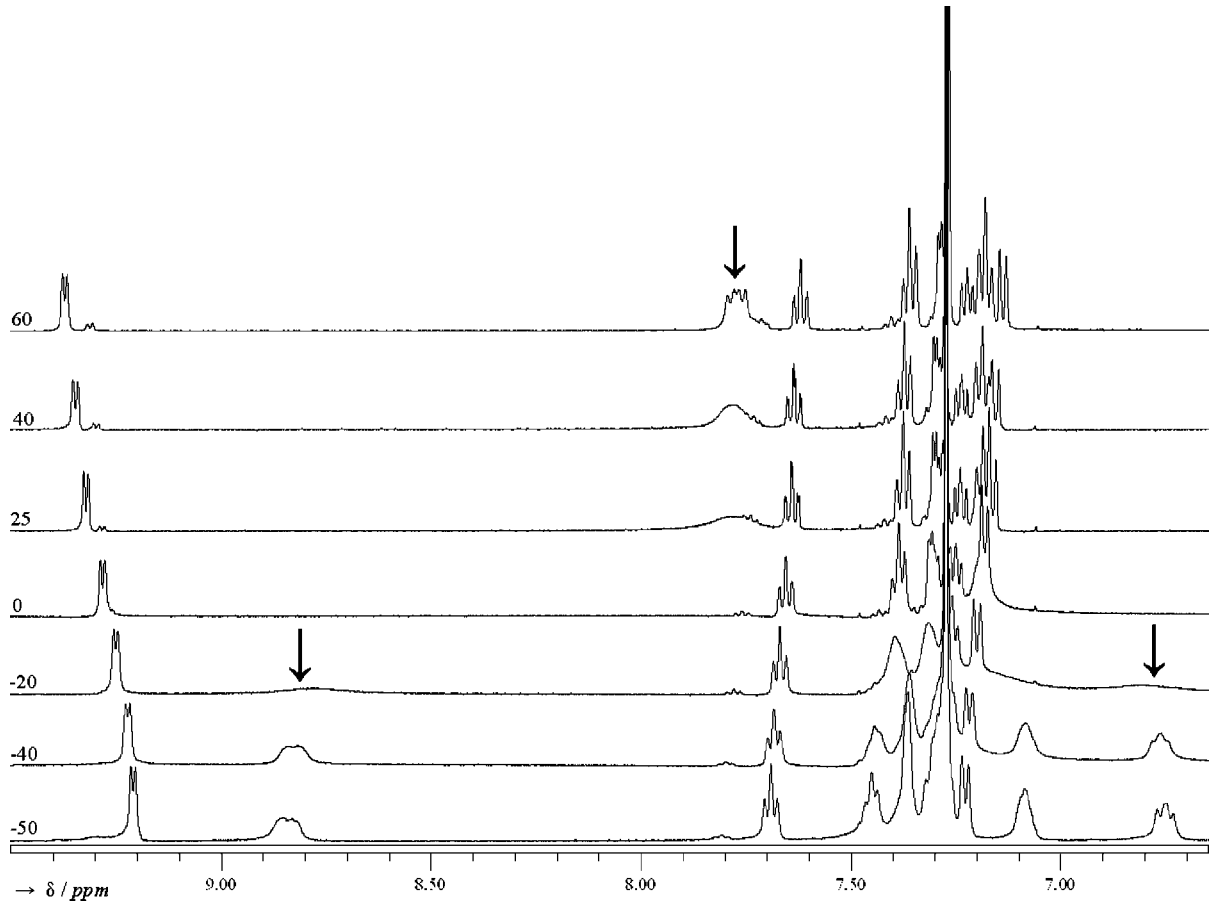

Figure 3. Aromatic region of the ^{1}H NMR spectra of compound **5a** at different temperatures (°C) recorded in $CDCl_3$. The arrows indicate the signals for the *ortho*-aryl protons.

Chart 2

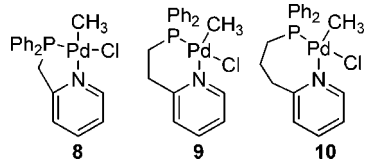

short Pd···H13 distance of 2.77 Å. The hydrogen atom is in a pseudoaxial position and shows an anagostic interaction with palladium, as was also revealed in the NMR spectra of the complex in solution (see above). The bond length and angle

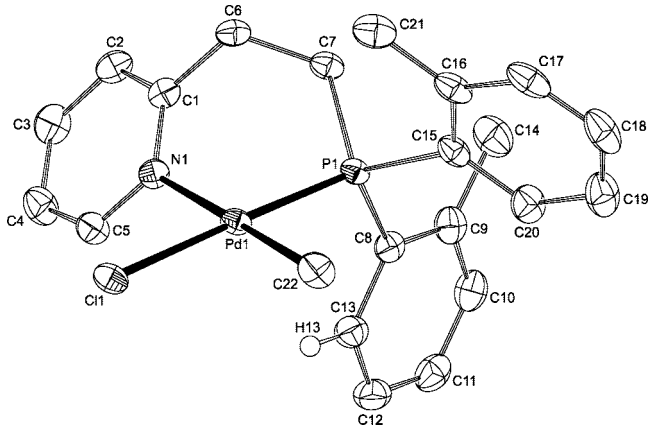

Figure 4. Displacement ellipsoid plot of **5a** in the crystal, drawn at the 50% probability level. Hydrogen atoms (except H13) and disordered solvent molecules are omitted for clarity.

Table 3. Selected Angles (deg) and Bond Lengths (Å) in Complex 5a[a]

P1−Pd1−N1	89.77(4)	Pd1−N1−C1	123.02(11)
P1−Pd1−Cl1	178.675(15)	N1−C1−C6	117.72(15)
P1−Pd1−C22	88.97(6)	C1−C6−C7	112.11(14)
N1−Pd1−Cl1	91.08(4)	C6−C7−P1	114.02(12)
N1−Pd1−C22	177.57(7)	C7−P1−Pd1	108.74(6)
Cl1−Pd1−C22	90.13(6)	C13−H13···Pd1	123
Pd1−P1	2.2305(6)	N1−C1	1.352(2)
Pd1−N1	2.1687(14)	C1−C6	1.505(2)
Pd1−Cl1	2.3796(6)	P1−C7	1.8493(17)
Pd1−C22	2.0487(17)	C6−C7	1.536(2)
Pd1···H13	2.77		

[a] Hydrogen atoms were introduced in calculated positions and refined with a riding model (see Experimental Section).

associated with this interaction are within the values usually found for this type of interaction.[15] In the solid state structure of the related palladium complex **9** (see Chart 2) a similar interactions was not observed; the shortest corresponding Pd···H distance was 3.09 Å´.[9]

We have also obtained the crystal structure of **5b**; it is shown in fFigure 5, and selected bond lengths and angles are given in Table 4. The structure is similar to that of **5a**: the metallocycle has a "boat" conformation and has a slightly distorted square-planar geometry of the palladium atom, with a *cis* orientation of the phosphorus atom and the methyl group. The oxygen atoms have no interaction with the palladium atom, as shown by the shortest Pd···O distance of 3.5845(18)Å. One *ortho*-aryl proton shows an anagostic interaction with palladium: H13 is in a pseudoaxial position of the metal, with a short Pd···H13 distance of 2.92 Å. These findings were corroborated by the NMR studies in the solution phase (see above).

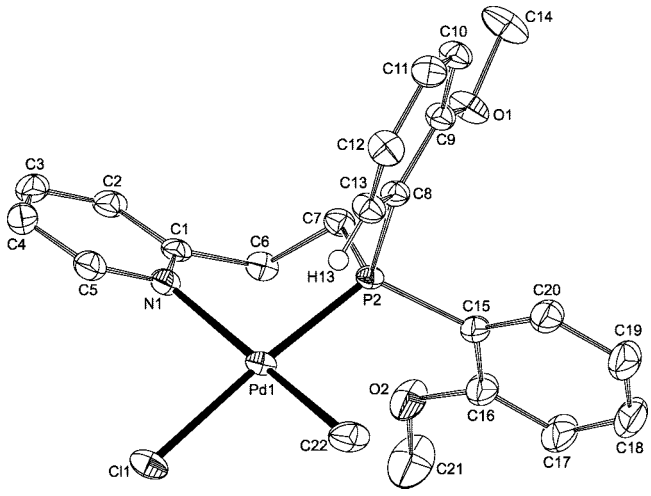

Figure 5. Displacement ellipsoid plot of **5b** in the crystal, drawn at the 50% probability level. Hydrogen atoms (except H13) and disordered solvent molecules are omitted for clarity.

Table 4. Selected Angles (deg) and Bond Lengths (Å) in Complex 5b[a]

P2−Pd1−N1	92.22(4)	Pd1−N1−C1	123.03(13)
P2−Pd1−Cl1	175.035(17)	N1−C1−C6	117.86(16)
P2−Pd1−C22	88.68(7)	C1−C6−C7	112.94(15)
N1−Pd1−Cl1	89.45(4)	C6−C7−P2	113.13(13)
N1−Pd1−C22	176.44(8)	C7−P2−Pd1	108.69(6)
Cl1−Pd1−C22	89.94(7)	C13−H13···Pd1	119
Pd1−P2	2.2177(6)	N1−C1	1.350(2)
Pd1−N1	2.1644(17)	C1−C6	1.497(3)
Pd1−Cl1	2.3794(6)	P2−C7	1.8412(19)
Pd1−C22	2.047(2)	C6−C7	1.544(3)
Pd1···O2	3.5845(18)	Pd1···H13	2.92

[a] Hydrogen atoms were introduced in calculated positions and refined with a riding model (see Experimental Section).

Scheme 4. Synthesis of Cationic Palladium Complexes 6

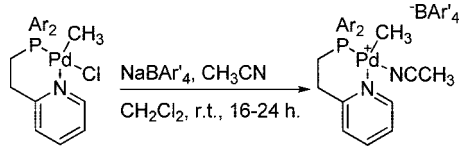

5a-c

6a, 94%
6b, 87%
6c, 83%

Synthesis and Characterization of Cationic Palladium Complexes. We obtained the cationic palladium complexes **6** from reaction of their neutral precursors with $NaBAr'_4$ [Ar′ = 3,5-di(trifluoromethyl)phenyl]; see Scheme 4. After workup, the pure products were obtained as white solids in high yields.

In analogy with their neutral precursors, complexes **6a** and **6b** exhibited slow inversion of the six-membered metallocycle, as indicated by the appearance of broad signals in the room-temperature ^{1}H NMR spectra (measured in CD_2Cl_2). When the samples were cooled to −40 °C, the signals became even broader and sharp separate signals for inequivalent aromatic or methylene protons could not be observed. Due to practical limitations, we did not cool the samples to a temperature at which the separate signals could be observed. When the temperature was raised, the signals became sharper. At 80 °C (in $CDCl_2CDCl_2$ solution), all peaks in the spectra of compounds **6a** and **6b** appeared sharp.

Complex **6c** did not show broad signals at room temperature, and the aryl groups and methylene protons were equivalent. This shows that ring inversion of this complex is fast on the NMR time scale at ambient temperature, just like that of its precursor **5c**.

Table 5. Ethene Oligomerization Using 4a−c and 7 as Catalyst Precursors[a]

complex	productivity (g C_2H_4/(mol Ni · h))	TOF[b]	product distribution (%)[c] C4	C6	C8	C10	>C10	1-butene (%)[d]
4a	46×10^4	16×10^3	78	7	5	4	6	76
4b	182×10^4	65×10^3	95	4	<1			46
4c	38×10^4	14×10^3	93	7	<1			90
7	196×10^4	70×10^3	86	11	3	<1		18

[a] Conditions: 10 μmol of nickel complex, MAO activator (Al/Ni = 230), 10 bar of ethene, 1.0 mmol of heptane (internal standard), toluene solvent, total volume: 25 mL, *T*: 30 °C, time: 30 min. [b] Turnover frequency in (mol C_2H_4)·(mol Ni·h)$^{-1}$. [c] Mol percentage of combined C*n* products. [d] As percentage of total C4 fraction.

Nickel-Catalyzed Ethene Oligomerization. Nickel complexes of pyridine-phosphine ligands have been applied successfully in the oligomerization of ethene.[2,6,7,9,10] We studied the behavior of nickel complexes **4** as catalyst precursors in this reaction. The complexes were activated by MAO, and catalytic runs were performed in toluene at 30 °C for 30 min. The results of the catalytic studies are summarized in Table 5. For comparison, the results we have previously obtained with complex **7** (see Chart 1) are included as well.[9]

As can be seen from the table, complexes **4** form active catalysts after MAO activation. They were most active during the first 5 to 10 min of a run, as evident from the amount of cooling necessary to maintain the desired temperature of the exothermic reaction. Butenes are the main products in all cases, with a maximum selectivity of 95% for **4b**. Complex **4a** produces a significant amount of higher olefins, while **4b** and **4c** can be regarded as dimerization catalysts. The influence of the different aromatic P-substituents is apparent from the different catalytic behavior of complexes **4a−c** and **7**. Whereas the selectivity for 1-butene within the butenes fraction is low for complex **7**, which has phenyl substituents at phosphorus, the larger aromatic groups in **4** cause the formation of a higher percentage of 1-butene. Especially **4c** shows a high selectivity of 90%. Apparently the bulky mesityl substituents prevent isomerization of the growing oligomer chain. This can be rationalized by considering the fact that a branched alkyl chain, formed after isomerization, requires more space around the metal center than a linear chain, which can bend away from this center. The formation of branched alkyl chains is therefore disfavored in the case of the bulky mesityl substituents at phosphorus. This is accompanied by a decrease in activity, as compared to the catalytic behavior of phenyl-substituted **7**.

The 2-tolyl substituents in **4a** cause a similar, but less strong effect than **4c**. This explains the 1-butene selectivity and activity of this complex. Catalyst precursor **4b** deviates from this trend. The electronic properties of this complex are expected to be similar to those of **4c**, and the electronic properties cannot explain the lower 1-butene selectivity and higher activity of **4b**. Possibly, an interaction of the methoxy oxygen atoms causes the different catalytic behavior. No Pd···O interaction was observed in the crystal structure of palladium complex **5b**, but this might be different for the catalytically active, cationic species formed from **4b**. A different behavior in ethene oligomerization for a palladium complex of an anisyl-substituted

Table 6. Ethene Oligomerization Using 6a−c as Catalyst Precursors[a]

		product distribution (%)[c]							
complex	TOF[b]	C4	C5	C6	C7	C8	C9	C10	>C10
6a	6	47	8	10	4	8	1	6	15
6b	25	41	3	11	1	10	<1	9	24
6c	8	63	9	6	4	5	2	4	6

[a] Conditions: 100 μmol of palladium complex, 10 bar of ethene, 0.10 mmol of heptane (internal standard), toluene solvent, total volume: 25 mL, *T*: 30 °C, time: 120 min. [b] Turnover frequency in (mol C_2H_4)·(mol Pd·h)$^{-1}$. [c] Mol percentage of combined C*n* products.

ligand, as compared to complexes of related alkyl-substituted ligands, has been observed before.[17]

Palladium-Catalyzed Ethene Oligomerization. Palladium complexes of P,N ligands have been tested for ethene oligomerization activity much less frequently than their nickel counterparts. They have been reported to be active in ethene oligomerization,[8,16a,17,18] although no or very low activity in this reaction has often been observed as well with these complexes.[7,9,10,19] Only one report describes an active catalyst containing a pyridine-phosphine ligand,[8] whereas other systems showed no or very low activity.[7,9,10] We tested complexes **6** for productivity in the oligomerization of ethene, and the results are summarized in Table 6.

As can be seen from the table, the complexes all have a very low productivity. Like their nickel counterparts, the complex containing ligand **1b** forms the most active catalyst. Next to butenes, a significant amount of higher oligomers is formed as well. This is in contrast to the catalytic behavior of related complexes.[9,10] The oligomers with an odd number of carbons in the chain originate from the first chain growing from the catalyst precursor, which starts from a methylpalladium species. After β-hydride elimination, a palladium hydride species is formed, and only chains with an even number of carbons are formed henceforth. As a consequence, the catalyst with the highest turnover number (**6b**) has the lowest percentage of oligomers with an odd number of carbons.

Conclusions

The new pyridine-phosphine ligands **1** were used for the preparation of nickel and palladium complexes. The nickel complexes **4** all have a distorted tetrahedral geometry of the metal center and are consequently paramagnetic. The neutral palladium complexes **5** have a distorted square-planar geometry around the metal. In complexes **5a** and **5b**, the inversion of the six-membered metallocycle is hindered. This phenomenon is probably related to an anagostic C−H···Pd interaction of a proton of the ligand with the axial position of the palladium atom. The interaction was apparent from the crystal structures and low-temperature NMR spectra of the complexes. Complex **5c** does not exhibit hindered inversion of the palladium chelate ring nor any Pd···H interactions. The cationic palladium complexes **6** show similar coordination behavior to their neutral precursors, with square-planar surrounded metal centers, and hindered ring inversion for **6a** and **6b**.

After MAO activation the nickel complexes form active catalysts for the oligomerization of ethene. The bulky mesityl and 2-tolyl phosphorus substituents in **4a** and **4c** disfavor isomerization of the oligomer chain, as shown by a high 1-butene selectivity. This becomes evident from the comparison with the catalytic behavior of earlier reported complex **7**, in which the corresponding substituents are phenyl groups. The higher 1-butene selectivity is accompanied by a lower productivity. The catalytic behavior of the complex formed after activation of **4b**, containing the anisyl-substituted ligand, is different from that of the other complexes. An interaction of the methoxy oxygen with the nickel center might be the reason for this. The cationic palladium complexes **6** show a very low activity in ethene oligomerization. Selectivity for butenes is much lower than for their nickel counterparts, and significant amounts of higher oligomers are formed.

Experimental Part

General experimental information is given in the Supporting Information. The following abbreviations are used: py = pyridyl, tol = tolyl, anis = anisyl, mes = mesityl, Ar′ = 3,5-di(trifluoromethyl)phenyl.

Materials. Solvents were dried and distilled under dinitrogen; acetonitrile, CH_2Cl_2, CD_2Cl_2, and $CDCl_3$ from CaH_2, toluene from sodium, Et_2O and THF from sodium/benzophenone, and pentane and hexanes from sodium/benzophenone/triglyme. Toluene and heptane in toluene solution used for nickel-catalyzed oligomerization were stored over sodium/potassium alloy. Phenylsilane and 2-vinylpyridine (**2**) were distilled under dinitrogen. Di-2-tolylphosphine oxide,[11] di-2-anisylphosphine oxide,[12] dimesitylphosphine oxide,[11] $(DME)NiCl_2$,[20] $(COD)Pd(CH_3)Cl$,[21] and $NaBAr'_4$[22] were synthesized according to the published procedures. All other chemicals were purchased from commercial suppliers and used as received.

X-ray Crystal Structure Determinations. X-ray reflections were measured with Mo Kα radiation ($\lambda = 0.71073$ Å) on a Nonius KappaCCD diffractometer with rotating anode. The structures were solved with direct methods (SHELXS-97[23] program for **4a**; SHELXS-86[23] program for **4c** and **5b**) or automated Patterson methods (DIRDIF-99[24] program for **5a**). Refinement was performed with SHELXL-97[23] against F^2 of all reflections. Non-hydrogen atoms were refined with anisotropic displacement parameters. All hydrogen atoms were introduced in calculated positions and refined with a riding model.

In **4a** the methyl group at C14 was refined with two orientations.

The crystals of **5a** and **5b** contained a large void, respectively (118 Å^3/unit cell for **5a**; 285 Å^3/unit cell for **5b**) filled with disordered solvent molecules. Their contribution to the structure factors was secured by back-Fourier transformation using the routine SQUEEZE of the program PLATON,[25] resulting in 34 electrons/unit cell for **5a** and 35 electrons/unit cell for **5b**.

Geometry calculations and checking for higher symmetry was performed with the PLATON[25] program. Further details about the crystal structure determinations are given in Table 7.

(17) Keim, W.; Killat, S.; Nobile, C. F.; Suranna, G. P.; Englert, U.; Wang, R. M.; Mecking, S.; Schroder, D. L. *J. Organomet. Chem.* **2002**, *662*, 150–171.

(18) (a) Daugulis, O.; Brookhart, M. *Organometallics* **2002**, *21*, 5926–5934. (b) van den Beuken, E. K.; Smeets, W. J. J.; Spek, A. L.; Feringa, B. L. *Chem. Commun.* **1998**, 223–224.

(19) (a) Anderson, C. E.; Batsanov, A. S.; Dyer, P. W.; Fawcett, J.; Howard, J. A. K. *Dalton Trans.* **2006**, 5362–5378. (b) Guan, Z. B.; Marshall, W. J. *Organometallics* **2002**, *21*, 3580–3586. (c) Shi, P. Y.; Liu, Y. H.; Peng, S. M.; Liu, S. T. *Organometallics* **2002**, *21*, 3203–3207. (d) Sirbu, D.; Consiglio, G.; Gischig, S. *J. Organomet. Chem.* **2006**, *691*, 1143–1150.

(20) Ward, L. G. L. *Inorg. Synth.* **1971**, *13*, 154–64.

(21) Rulke, R. E.; Ernsting, J. M.; Spek, A. L.; Elsevier, C. J.; Van Leeuwen, P. W. N. M.; Vrieze, K. *Inorg. Chem.* **1993**, *32*, 5769–5778.

(22) Brookhart, M.; Grant, B.; Volpe, A. F. *Organometallics* **1992**, *11*, 3920–3922.

(23) Sheldrick, G. *Acta Crystallogr., Sect. A* **2008**, *64*, 112–122.

(24) Beurskens, P. T.; Admiraal, G.; Beurskens, G.; Bosman, W. P.; Garcia-Granda, S.; Gould, R. O.; Smits, J. M. M.; Smykalla, C. *The DIRDIF99 Program System*, Technical Report of the Crystallography Laboratory; University of Nijmegen: The Netherlands; 1999.

(25) Spek, A. L. *J. Appl. Crystallogr.* **2003**, *36*, 7–13.

Table 7. Selected Crystallographic Data for Complexes 4a, 4c, 5a, and 5b

	4a	4c	5a	5b
formula	$C_{21}H_{22}Cl_2NNiP$	$C_{25}H_{30}Cl_2NNiP$	$C_{22}H_{25}ClNPPd$ + disordered solvent	$C_{22}H_{25}ClNO_2PPd$ + disordered solvent
fw	448.98	505.08	476.25[a]	508.25[a]
cryst color	purple	purple	colorless	colorless
cryst size [mm^3]	0.36 × 0.21 × 0.15	0.35 × 0.03 × 0.01	0.25 × 0.10 × 0.10	0.30 × 0.15 × 0.10
temp [K]	150	100	150	150
cryst syst	monoclinic	monoclinic	triclinic	triclinic
space group	$P2_1/c$ (no. 14)	$P2_1/c$ (no. 14)	$P\bar{1}$ (no. 2)	$P\bar{1}$ (no. 2)
a [Å]	9.3096(1)	16.490(2)	8.6654(10)	8.3871(10)
b [Å]	20.1793(2)	10.2308(12)	11.1373(10)	12.376(2)
c [Å]	13.9525(2)	14.870(2)	12.839(2)	13.626(2)
α [deg]	90	90	74.356(15)	103.680(15)
β [deg]	129.6543(4)	101.206(12)	73.078(15)	106.062(18)
γ [deg]	90	90	68.916(18)	99.75(2)
V [Å^3]	2018.03(4)	2460.8(5)	1087.0(3)	1278.2(4)
Z	4	4	2	2
D_x [g/cm^3]	1.478	1.363	1.455[a]	1.321[a]
$(\sin\theta/\lambda)_{max}$ [Å^{-1}]	0.65	0.60	0.65	0.65
reflns measd/unique	34 570/4606	33 780/4445	30 812/4982	26 835/5829
μ [mm^{-1}]	1.310	1.083	1.055[a]	0.908[a]
abs corr	multiscan	none	none	none
abs corr range	0.56−0.82			
params/restraints	238/0	277/0	238/0	257/0
R1/wR2 [$I > 2\sigma(I)$]	0.0261/0.0574	0.0795/0.1477	0.0223/0.0562	0.0251/0.0731
R1/wR2 [all reflns]	0.0350/0.0610	0.1530/0.1746	0.0256/0.0573	0.0267/0.0741
S	1.026	1.084	1.060	1.102
resid density [e/Å^3]	−0.31/0.33	−0.61/0.77	−0.86/0.49	−0.67/0.59

[a] Derived parameters do not contain the contribution of the disordered solvent.

2-[2-(Di-2-tolylphosphinoyl)ethyl]pyridine (3a). Di-2-tolylphosphine oxide (1.07 g, 4.63 mmol, 1.0 equiv) and 2-vinylpyridine (**2**) (0.487 g, 4.63 mmol, 1.0 equiv) were dissolved in 25 mL of THF. KOtBu (26 mg, 0.23 mmol, 0.05 equiv) was added, and the mixture was stirred at 60 °C for 16 h. Water (5 mL) was added, and the mixture was concentrated in vacuo. EtOAc (100 mL) was added, and the solution was washed with water twice and with brine, dried over $MgSO_4$, and concentrated in vacuo to yield a colorless oil. The product was precipitated by addition of Et_2O (20 mL), filtrated, washed with Et_2O, and dried in vacuo to yield the product as a white solid (1.24 g, 3.69 mmol, 80%, mp 120 °C). ^{1}H NMR δ (500 MHz, $CDCl_3$) ppm: 8.50−8.48 (m, 1H, py-H6), 7.80 (ddd, J = 12.8, 7.7, 1.0 Hz, 2H, tol-H6), 7.56 (dt, J = 7.7, 1.3 Hz, 1H, py-H4), 7.39−7.35 (m, 2H, tol-H4), 7.29−7.25 (m, 2H, tol-H5), 7.17−7.13 (m, 3H, py-H3 + tol-H3), 7.12−7.08 (m, 1H, py-H5), 3.16−3.10 (m, 2H, py-CH_2), 2.92−2.86 (m, 2H, P−CH_2), 2.30 (s, 6H, CH_3). ^{13}C{^{1}H} NMR δ (125 MHz, $CDCl_3$) ppm: 160.6 (d, J = 14.3 Hz, py-C2), 149.4 (s, py-C6), 141.7 (d, J = 8.6 Hz, tol-C2), 136.6 (s, CH), 132.2 (d, J = 10.4 Hz, CH), 132.0 (s, CH), 131.9 (s, CH), 131.8 (s, CH), 131.4 (d, J = 95.5 Hz, tol-C1), 125.8 (d, J = 11.8 Hz, CH), 123.2 (s, CH), 121.5 (s, CH), 30.0 (d, J = 2.2 Hz, py-*C*H$_2$), 28.6 (d, J = 71.6 Hz, P-*C*H$_2$), 21.4 (d, J = 4.3 Hz, *C*H$_3$). ^{31}P{^{1}H} NMR δ (121 MHz, $CDCl_3$) ppm: 34.6. Anal. Calcd for $C_{21}H_{22}NOP$: C, 75.21; H, 6.61; N, 4.18. Found: C, 75.06; H, 6.70; N, 4.06. HRMS (FAB) m/z: calcd for $C_{21}H_{23}NOP$ [M + H]$^+$ 336.1517; found 336.1505.

2-[2-(Di-2-anisylphosphinoyl)ethyl]pyridine (3b). Di-2-anisylphosphine oxide (2.49 g, 9.49 mmol, 1.0 equiv) and 2-vinylpyridine (**2**) (1.00 mL, 9.49 mmol, 1.0 equiv) were dissolved in 50 mL of THF. KOtBu (0.11 g, 0.95 mmol, 0.1 equiv) was added, and the mixture was stirred at 60 °C for 16 h, after which unlocked ^{31}P NMR showed full conversion. Water (10 mL) was added, and the mixture was concentrated in vacuo. It was redissolved in EtOAc (200 mL) and washed with water twice and with brine. After drying over $MgSO_4$ and concentration in vacuo, column chromatography (eluent 5% MeOH in CH_2Cl_2) yielded the product as a white solid (2.52 g, 6.87 mmol, 72%, mp 67 °C). ^{1}H NMR δ (500 MHz, $CDCl_3$) ppm: 8.45 (d, J = 4.3 Hz, 1H, py-H6), 7.64 (ddd, J = 13.4, 7.5, 1.6 Hz, 2H, anis-H6), 7.52 (dt, J = 7.7, 1.5 Hz, 1H, py-H4), 7.46−7.42 (m, 2H, anis-H4), 7.14 (d, J = 7.7 Hz, 1H, py-H3), 7.09−7.05 (m, 1H, py-H5), 7.02−6.97 (m, 2H, anis-H5), 6.85 (dd, J = 8.3, 5.2 Hz, 2H, anis-H3), 3.70 (s, 6H, CH_3), 3.12−3.05 (m, 2H, py-CH_2), 3.05−2.97 (m, 2H, P−CH_2). ^{13}C{^{1}H} NMR δ (75 MHz, $CDCl_3$) ppm: 161.5 (d, J = 15.3 Hz, py-C2), 160.7 (s, anis-C2), 149.1 (s, py-C6), 136.3 (s, CH), 134.1 (d, J = 6.5 Hz, CH), 133.5 (s, CH), 123.0 (s, CH), 121.2 (s, CH), 120.9 (d, J = 100.6 Hz, anis-C1), 120.7 (d, J = 11.3 Hz, CH), 110.9 (d, J = 5.9 Hz, CH), 55.5 (s, *C*H$_3$), 30.5 (s, py-*C*H$_2$), 29.2 (d, J = 74.4 Hz, P-*C*H$_2$). ^{31}P{^{1}H} NMR δ (121 MHz, $CDCl_3$) ppm: 33.7. Anal. Calcd for $C_{21}H_{22}NO_3P$: C, 68.66; H, 6.04; N, 3.81. Found: C, 68.52; H, 5.94, N, 3.72. HRMS (FAB) m/z: calcd for $C_{21}H_{23}NO_3P$ [M + H]$^+$ 368.1416; found 368.1417.

2-[2-(Dimesitylphosphinoyl)ethyl]pyridine (3c). Dimesitylphosphine oxide (0.425 g, 1.48 mmol, 1.0 equiv) and 2-vinylpyridine (**2**) (0.156 mL, 1.48 mmol, 1.0 equiv) were dissolved in 10 mL of THF. KOtBu (34 mg, 0.29 mmol, 0.2 equiv) was added, and the mixture was stirred at 60 °C for 16 h, after which unlocked ^{31}P NMR showed full conversion. Water (5 mL) was added, and the mixture was concentrated in vacuo. It was redissolved in 100 mL of EtOAc and washed with water twice and with brine. It was dried over $MgSO_4$ and concentrated in vacuo, after which column chromatography (eluent 5% MeOH in CH_2Cl_2) yielded the product as an off-white solid (0.361 g, 0.92 mmol, 62%, mp 158 °C). ^{1}H NMR δ (300 MHz, $CDCl_3$) ppm: 8.45 (d, J = 7.9 Hz, 1H, py-H6), 7.52 (dt, J = 7.7, 1.8 Hz, 1H, py-H4), 7.11 (d, J = 7.7 Hz, 1H, py-H3), 7.06 (m, 1H, py-H5), 6.77 (d, J = 3.4 Hz, 4H, mes-H3), 3.08−2.96 (m, 2H, py-CH_2), 2.92−2.82 (m, 2H, P-CH_2), 2.37 (s, 12H, mes-2-CH_3), 2.22 (s, 6H, mes-4-CH_3). ^{13}C{^{1}H} NMR δ (75 MHz, $CDCl_3$) ppm: 161.1 (d, J = 15.2 Hz, py-C2), 149.2 (s, py-C6), 141.4 (d, J = 9.8, mes-C2), 140.8 (s, mes-C4), 136.8 (s, CH), 131.3 (d, J = 10.7 Hz, mes-C3), 130.2 (d, J = 94.4 Hz, mes-C1), 123.3 (s, CH), 121.5 (s, CH), 35.8 (d, J = 66.3 Hz, P-*C*H$_2$), 31.2 (s, py-*C*H$_2$), 23.2 (s, mes-2-*C*H$_3$), 21.1 (s, mes-4-*C*H$_3$). ^{31}P{^{1}H} NMR δ (121 MHz, $CDCl_3$) ppm: 41.8. Anal. Calcd for $C_{25}H_{30}NOP$: C, 76.70; H, 7.72; N, 3.58. Found: C, 76.61; H, 7.78, N, 3.93. HRMS (FAB) m/z: calcd for $C_{25}H_{31}NOP$ [M + H]$^+$ 392.2143; found 392.2147.

2-[2-(Di-2-tolylphosphino)ethyl]pyridine (1a). 2-[2-(Di-2-tolylphosphinoyl)ethyl]pyridine (**3a**) (1.48 g, 4.41 mmol, 1.0 equiv) was dissolved in phenylsilane (8.0 mL, 65 mmol, 15 equiv), and

the mixture was refluxed overnight, after which unlocked ^{31}P NMR showed full conversion. The mixture was concentrated in vacuo and co-evaporated with three times with 5 mL of toluene. The product was purified using column chromatography using Et_2O as the eluent and a second column with CH_2Cl_2 as the eluent to yield the product as a yellowish oil (1.33 g, 4.18 mmol, 95%). ^{1}H NMR δ (500 MHz, $CDCl_3$) ppm: 8.50−8.48 (d, J = 4.4 Hz, 1H, py-H6), 7.58 (dt, J = 7.7, 1.8 Hz, 1H, py-H4), 7.29−7.26 (m, 2H, tol-H4), 7.25−7.21 (m, 2H, tol-H6), 7.19−7.14 (m, 4H, tol-H3 + -H5), 7.14−7.09 (m, 2H, py-H3 + -H5), 2.97−2.92 (m, 2H, py-CH_2), 2.48−2.44 (m, 2H, P-CH_2), 2.45 (s, 6H, CH_3). ^{13}C{^{1}H} NMR δ (125 MHz, $CDCl_3$) ppm: 162.2 (d, J = 13.9 Hz, py-C2), 149.5 (s, py-C6), 142.5 (d, J = 25.2 Hz, tol-C2), 136.9 (d, J = 13.5 Hz, tol-C1), 136.5 (s, CH), 131.3 (s, CH), 130.2 (d, J = 4.6 Hz, CH), 128.6 (s, CH), 126.3 (s, CH), 122.8 (s, CH), 121.4 (s, CH), 34.7 (d, J = 18.6 Hz, py-*C*H_2), 27.1 (d, J = 12.7 Hz, P-*C*H_2), 21.4 (d, J = 21.1 Hz, *C*H_3). ^{31}P{^{1}H} NMR δ (121 MHz, $CDCl_3$) ppm: −35.8. Anal. Calcd for $C_{21}H_{22}NP$: C, 78.97; H, 6.94; N, 4.39. Found: C, 78.88; H, 6.87, N, 4.31. MS (EI) *m*/*z* (rel intensity): 319 (8) $[M]^{+\bullet}$, 228 (100) $[M - tol]^+$, 106 (10) $[M - P(tol)_2]^+$.

2-[2-(Di-2-anisylphosphino)ethyl]pyridine (1b). 2-[2-(Di-2-anisylphosphinoyl)ethyl]pyridine (**3b**) (137 mg, 0.37 mmol, 1.0 equiv) was dissolved in phenylsilane (2.0 mL, 16.2 mmol, 43 equiv), and the mixture was refluxed overnight, after which unlocked ^{31}P NMR showed full conversion. The mixture was concentrated and purified by column chromatography with CH_2Cl_2 → 5% MeOH/CH_2Cl_2 as the eluent to yield the product as a white solid (122 mg, 0.35 mmol, 93%, mp 47 °C). ^{1}H NMR δ (500 MHz, $CDCl_3$) ppm: 8.53 (d, J = 4.7 Hz, 1H, py-H6), 7.58 (t, J = 7.6 Hz, 1H, py-H4), 7.34−7.30 (m, 2H, anis-H4), 7.21−7.16 (m, 3H, py-H3 + anis-H6), 7.12−7.09 (m, 1H, py-H5), 6.93 (t, J = 7.4 Hz, 2H, anis-H5), 6.87 (dd, J = 8.1, 4.1 Hz, 2H, anis-H3), 3.80 (s, 6H, CH_3), 3.01−2.94 (m, 2H, py-CH_2), 2.55−2.50 (m, 2H, P-CH_2). ^{13}C{^{1}H} NMR δ (125 MHz, $CDCl_3$) ppm: 162.7 (d, J = 13.6 Hz, py-C2), 161.7 (d, J = 13.5 Hz, anis-C2), 149.3 (s, py-C6), 136.4 (s, CH), 132.9 (d, J = 5.1 Hz, CH), 130.0 (s, CH), 125.7 (d, J = 15.2 Hz, anis-C1), 122.8 (s, CH), 121.1 (s, CH), 121.0 (d, J = 2.1 Hz, CH), 110.4 (s, CH), 55.7 (s, *C*H_3), 35.2 (d, J = 18.6 Hz, py-*C*H_2), 25.1 (d, J = 13.1 Hz, P-*C*H_2). ^{31}P{^{1}H} NMR δ (121 MHz, $CDCl_3$) ppm: −34.6. Anal. Calcd for $C_{21}H_{22}NO_2P$: C, 71.78; H, 6.31; N, 3.99. Found: C, 71.64; H, 6.27, N, 3.84. MS (EI) *m*/*z* (rel intensity): 351 (18) $[M]^{+\bullet}$, 244 (100) $[M - anis]^+$, 137 (7) $[M - 2anis]^+$, 136 (7) $[M - 2anis - H]^+$, 107 (13) $[anis]^+$, 106 (12) $[M - P(anis)_2]^+$.

2-[2-(Dimesitylphosphino)ethyl]pyridine (1c). 2-[2-(Dimesitylphosphinoyl)ethyl]pyridine (**3c**) (205 mg, 0.52 mmol, 1.0 equiv) was dissolved in phenylsilane (4.0 mL, 32 mmol, 62 equiv), and the mixture was refluxed overnight, after which unlocked ^{31}P NMR showed full conversion. The mixture was concentrated in vacuo and purified by column chromotagraphy with CH_2Cl_2 → 5% MeOH/CH_2Cl_2 as the eluent. After co-evaporation with hexanes (5 × 5 mL), the product was obtained as a white solid (196 mg, 0.52 mmol, 100%, mp 83 °C). ^{1}H NMR δ (500 MHz, $CDCl_3$) ppm: 8.51 (d, J = 4.2 Hz, 1H, py-H6), 7.56 (dt, J = 7.7, 1.8 Hz, 1H, py-H4), 7.11−7.06 (m, 2H, py-H3 + -H5), 6.78 (d, J = 2.1 Hz, 2H, mes-H3), 2.94−2.89 (m, 2H, py-CH_2), 2.80−2.74 (m, 2H, P−CH_2), 2.31 (s, 12H, mes-2-CH_3), 2.24 (s, 6H, mes-4-CH_3). ^{13}C{^{1}H} NMR δ (125 MHz, $CDCl_3$) ppm: 162.5 (d, J = 16.8 Hz, py-C2), 149.4 (s, py-C6), 142.1 (d, J = 13.6 Hz, mes-C2), 137.5 (s, mes-C4), 136.5 (s, CH), 133.1 (d, J = 21.5 Hz, mes-C1), 130.1 (d, J = 3.0 Hz, mes-C3), 122.7 (s, CH), 121.2 (s, CH), 36.1 (d, J = 22.7 Hz, py-*C*H_2), 31.2 (d, J = 16.0 Hz, P-*C*H_2), 23.4 (d, J = 13.1 Hz, mes-2-*C*H_3), 21.0 (s, mes-4-*C*H_3). ^{31}P{^{1}H} NMR δ (121 MHz, $CDCl_3$) ppm: −20.8. Anal. Calcd for $C_{25}H_{30}NP$: C, 79.97; H, 8.05; N, 3.73. Found: C, 80.11; H, 7.98, N, 3.65. MS (EI) *m*/*z* (rel intensity): 375 (10) $[M]^{+\bullet}$, 360 (100) $[M - CH_3]$, 256 (89) $[M - mes]^+$, 138 (25) $[M - 2mes + H]^+$, 106 (37) $[M - P(mes)_2]^+$.

2-[2-(Di-2-tolylphosphino)ethyl]pyridinenickel Dichloride (4a). A mixture of 2-[2-(di-2-tolylphosphino)ethyl]pyridine (**1a**) (215 mg, 0.67 mmol, 1.0 equiv), (DME)$NiCl_2$ (148 mg, 0.67 mmol, 1.0 equiv), and CH_2Cl_2 (8 mL) was stirred for 16 h. It was filtered through a pad of Celite, washed with CH_2Cl_2, and concentrated in vacuo. Et_2O (5 mL) was added, and the mixture was put in a sonication bath for 30 min. The solids were filtered off, washed with Et_2O, and dried in vacuo to yield the product as a purple solid (175 mg, 0.39 mmol, 58%, mp 254 °C dec). Anal. Calcd for $C_{21}H_{22}Cl_2NNiP$: C, 56.18; H, 4.94; N, 3.12. Found: C, 55.99; H, 4.90, N, 2.96. HRMS (FAB) *m*/*z*: calcd for $C_{21}H_{22}ClNNiP$ $[M - Cl]^+$ 412.0532; found 412.0536. μ_{eff} = 3.85 μ_B.

2-[2-(Di-2-anisylphosphino)ethyl]pyridinenickel Dichloride (4b). A mixture of 2-[2-(di-2-anisylphosphino)ethyl]pyridine (**1b**) (114 mg, 0.32 mmol, 1.0 equiv), (DME)$NiCl_2$ (71 mg, 0.32 mmol, 1.0 equiv), and CH_2Cl_2 (5 mL) was stirred for 16 h. It was filtered through a pad of Celite, washed with CH_2Cl_2, and concentrated in vacuo. Et_2O (5 mL) was added, and the mixture was put in a sonication bath for 30 min. The solids were filtered off, washed with Et_2O, and dried in vacuo to yield the product as a brown solid (134 mg, 0.28 mmol, 86%, mp 235 °C dec). Anal. Calcd for $C_{21}H_{22}Cl_2NNiO_2P$: C, 52.44; H, 4.61; N, 2.91. Found: C, 52.53; H, 4.72, N, 2.85. HRMS (FAB) *m*/*z*: calcd for $C_{21}H_{22}ClNNiO_2P$ $[M - Cl]^+$ 444.0430; found 444.0426. μ_{eff} = 3.30 μ_B.

2-[2-(Dimesitylphosphino)ethyl]pyridinenickel Dichloride (4c). A mixture of 2-[2-(dimesitylphosphino)ethyl]pyridine (**1c**) (42 mg, 0.11 mmol, 1.0 equiv), (DME)$NiCl_2$ (25 mg, 0.11 mmol, 1.0 equiv), and CH_2Cl_2 (3 mL) was stirred for 16 h. It was filtered through a pad of Celite, washed with CH_2Cl_2, and concentrated in vacuo. Et_2O (3 mL) was added, and the mixture was put in a sonication bath for 30 min. The solids were filtered off, washed with Et_2O, and dried in vacuo to yield the product as a purple solid (38 mg, 0.075 mmol, 67%, mp 240 °C dec). Anal. Calcd for $C_{25}H_{30}Cl_2NNiP$: C, 59.45; H, 5.99; N, 2.77. Found: C, 59.36; H, 5.91, N, 2.71. HRMS (FAB) *m*/*z*: calcd for $C_{25}H_{30}ClNNiP$ $[M - Cl]^+$ 468.1158; found 468.1168. μ_{eff} = 3.30 μ_B.

2-[2-(Di-2-tolylphosphino)ethyl]pyridine Methylpalladium Chloride (5a). 2-[2-(Di-2-tolylphosphino)ethyl]pyridine (**1a**) (350 mg, 1.10 mmol, 1.0 equiv) and (COD)Pd(CH_3)Cl (291 mg, 1.10 mmol, 1.0 equiv) were dissolved in CH_2Cl_2 (20 mL), and the mixture was stirred for 16 h. Then, it was concentrated in vacuo to approximately 2 mL, after which 20 mL of Et_2O was added under vigorous stirring. The white precipitate was filtrated off and washed with Et_2O. Drying in vacuo yielded the product as a white solid (460 mg, 0.97 mmol, 88%, mp 227 °C dec). ^{1}H NMR δ (500 MHz, $CDCl_3$, 25 °C) ppm: 9.30 (dd, J = 5.4, 1.0 Hz, 1H, py-H6), 7.90−7.66 (bs, 2H, tol-H6), 7.63 (d pst, J = 7.7, 1.7 Hz, 1H, py-H4), 7.40−7.34 (m, 2H, tol-H4), 7.32−7.26 (m, 2H, tol-H3), 7.24−7.20 (m, 1H, py-H5), 7.20−7.14 (m, 3H, py-H3 + tol-H5), 3.50−3.42 (m, 2H, py-CH_2), 2.51 (s, 6H, CH_3), 2.49−2.43 (m, 2H, P-CH_2), 0.39 (d, J = 3.7 Hz, 3H, CH_3). ^{1}H NMR δ (500 MHz, $CDCl_3$, −50 °C) ppm: 9.21 (d, J = 5.3 Hz, 1H, py-H6), 8.86−8.82 (m, 1H, tol-H6), 7.71−7.67 (m, 1H, py-H4), 7.47−7.43 (m, 1H, tol-H4), 7.41−7.34 (m, 2H, tol′-H3 + -H4), 7.34−7.25 (m, 3H, py-H3 + tol-H3 + -H5), 7.23 (d, J = 7.6 Hz, 1H, py-H5), 7.11−7.04 (m, 1H, tol′-H5), 6.78−6.72 (m, 1H, tol′-H6), 3.73−3.3.65 (m, 1H, py-C*H*H), 3.36−3.24 (m, 1H, py-CH*H*), 2.84 (s, 3H, tol-CH_3), 2.71−2.63 (m, 1H, P-C*H*H), 2.21 (s, 3H, tol′-CH_3), 2.20−2.12 (m, 1H, P-CH*H*), 0.23 (d, J = 3.0 Hz, 3H, Pd-CH_3). ^{1}H NMR δ (500 MHz, $CDCl_3$, 60 °C) ppm: 9.37 (d, J = 5.5 Hz, 1H, py-H6), 7.77 (dd, J = 13.5, 7.8 Hz, 2H, tol-H6), 7.62 (d pst, J = 7.6, 1.5 Hz, 1H, py-H4), 7.38−7.34 (m, 2H, tol-H4), 7.30−7.26 (m, 2H, tol-H3), 7.24−7.21 (m, 1H, py-H5), 7.20−7.16 (m, 2H, tol-H5), 7.14 (d, J = 7.6 Hz, 1H, py-H3), 3.50−3.41 (m, 2H, py-CH_2), 2.53 (s, 6H, tol-CH_3), 2.49−2.45 (m, 2H, P-CH_2), 0.47 (d, J = 3.7 Hz, 3H, Pd-CH_3). ^{13}C{^{1}H} NMR δ (125 MHz, $CDCl_3$, 25 °C) ppm: 159.2 (d, J = 3.0 Hz, py-C2), 152.7 (s, py-C6), 140.8 (d, J = 6.3 Hz, tol-C2), 138.5 (s, CH),

137.0−136.1 (bs, CH), 132.2 (d, J = 7.6 Hz, CH), 131.4 (s, CH), 129.7 (d, J = 48.5 Hz, tol-C1), 126.1 (d, J = 12.7 Hz, CH), 124.1 (s, CH), 123.3 (s, CH), 36.7 (d, J = 6.8 Hz, py-*C*H_2), 25.5 (d, J = 29.1 Hz, P-*C*H_2), 23.5 (d, J = 5.9 Hz, tol-*C*H_3), 0.0 (s, Pd-*C*H_3). ^{31}P{^{1}H} NMR δ (121 MHz, $CDCl_3$, 25 °C) ppm: 40.3. Anal. Calcd for $C_{22}H_{25}ClNPPd$: C, 55.48; H, 5.29; N, 2.94. Found: C, 55.56; H, 5.22; N, 2.82. HRMS (FAB) *m*/*z*: calcd for $C_{22}H_{25}NPPd$ [M − Cl]$^+$ 440.0768; found 440.0756.

2-[2-(Di-2-anisylphosphino)ethyl]pyridine Methylpalladium Chloride (4b). 2-[2-(Di-2-anisylphosphino)ethyl]pyridine (**1b**) (332 mg, 0.95 mmol, 1.0 equiv) and (COD)Pd(CH_3)Cl (250 mg, 0.95 mmol, 1.0 equiv) were dissolved in CH_2Cl_2 (15 mL), and the mixture was stirred for 16 h. Then, it was concentrated in vacuo to approximately 1.5 mL, after which 15 mL of Et_2O was added under vigorous stirring. The white precipitate was filtrated off and washed with Et_2O. Drying in vacuo yielded the product as a white solid (436 mg, 0.86 mmol, 91%). ^{1}H NMR δ (500 MHz, $CDCl_3$, 25 °C) ppm: 9.35 (dd, J = 5.5, 1.1 Hz, 1H, py-H6), 7.64−7.60 (m, 1H, py-H4), 7.47−7.43 (m, 2H, anis-H4), 7.22−7.19 (m, 1H, py-H5), 7.14 (d, J = 7.7 Hz, 1H, py-H3), 6.96−6.92 (m, 4H, anis-H3 + -H5), 3.83 (s, 6H, anis-C*H*$_3$), 3.48−3.40 (m, 2H, py-C*H*$_2$), 2.41−2.38 (m, 2H, P-C*H*$_2$), 0.31 (d, J = 3.5 Hz, 3H, Pd-C*H*$_3$); *the signal for anis-H6 was not observed.* ^{1}H NMR δ (500 MHz, $CDCl_3$, −50 °C) ppm: 9.22 (d, J = 5.1 Hz, 1H, py-H6), 8.66 (dd, J = 16.5, 7.2 Hz, 1H, anis-H6), 7.68−7.64 (m, 1H, py-H4), 7.58−7.54 (m, 1H, anis-H4), 7.43−7.39 (m, 1H, anis′-H4), 7.24−7.20 (m, 2H, py-H3 + -H5), 7.10−7.07 (m, 1H, anis-H5), 7.01−6.98 (m, 1H, anis′-H3), 6.91 (d, J = 7.8 Hz, 1H, anis-H3), 6.82−6.78 (m, 1H, anis′-H5), 6.57−6.52 (dd, J = 11.5, 8.1 Hz, 1H, anis′-H6), 4.00 (s, 3H, anis-C*H*$_3$), 3.80−3.69 (m, 1H, py-C*H*H), 3.68 (s, 3H, anis′-C*H*$_3$), 3.25−3.12 (m, 1H, py-CH*H*), 2.79−2.72 (m, 1H, P-C*H*H), 2.01−1.92 (m, 1H, P-CH*H*), 0.17 (d, J = 3.5 Hz, 3H, Pd-C*H*$_3$). ^{1}H NMR δ (500 MHz, $CDCl_3$, 60 °C) ppm: 9.40 (d, J = 5.1 Hz, 1H, py-H6), 7.69−7.61 (m, 2H, anis-H6), 7.61−7.56 (m, 1H, py-H4), 7.44−7.39 (m, 2H, anis-H4), 7.20−7.16 (m, 1H, py-H5), 7.10 (d, J = 7.7 Hz, 1H, py-H3), 6.95−6.90 (m, 4H, anis-H3 + -H5), 3.81 (s, 6H, anis-C*H*$_3$), 3.45−3.34 (m, 2H, Py-C*H*$_2$), 2.44−2.37 (m, 2H, P-C*H*$_2$), 0.35 (d, J = 3.4 Hz, 3H, Pd-C*H*$_3$). ^{13}C{^{1}H} NMR δ (125 MHz, $CDCl_3$, 25 °C) ppm: 160.7 (d, J = 2.1 Hz, py-C2), 160.1 (s, anis-C2), 152.9 (s, py-C6), 138.1 (s, CH), 138−136 (bs, CH), 132.9 (s, CH), 123.9 (s, CH), 122.8 (s, CH), 120.7 (d, J = 12.2 Hz, CH), 119.2 (d, J = 51.9 Hz, anis-C1), 111.1 (d, J = 4.2 Hz, CH), 55.8 (s, anis-*C*H$_3$), 36.5 (d, J = 7.2 Hz, py-*C*H$_2$), 25.2 (d, J = 33.3 Hz, P-*C*H$_2$), −1.3 (s, Pd-*C*H$_3$). ^{13}C{^{1}H} NMR δ (125 MHz, $Cl_2DCCDCl_2$, 80 °C) ppm: 160.4 (d, J = 2.5 Hz, py-C2), 159.9 (s, anis-C2), 152.6 (s, py-C6), 137.6 (s, CH), 136.6 (d, J = 15.2 Hz, CH), 132.5 (s, CH), 123.5 (s, CH), 122.1 (s, CH), 120.4 (d, J = 12.2 Hz, CH), 119.2 (d, J = 51.1 Hz, anis-C1), 111.2 (d, J = 4.7 Hz, CH), 55.5 (s, anis-*C*H$_3$), 36.0 (d, J = 6.8 Hz, py-*C*H$_2$), 24.9 (d, J = 32.9 Hz, P-*C*H$_2$), −1.9 (s, Pd-*C*H$_3$). ^{31}P{^{1}H} NMR δ (121 MHz, $CDCl_3$, 25 °C) ppm: 37.5. Anal. Calcd for $C_{22}H_{25}ClNO_2PPd$: C, 51.99; H, 4.96; N, 2.76. Found: C, 51.84; H, 5.08; N, 2.64. HRMS (FAB) *m*/*z*: calcd for $C_{22}H_{25}NO_2PPd$ [M − Cl]$^+$ 472.0667; found 472.0661.

2-[2-(Dimesitylphosphino)ethyl]pyridine Methylpalladium Chloride (5c). 2-[2-(Dimesitylphosphino)ethyl]pyridine (**1c**) (100 mg, 0.27 mmol, 1.0 equiv) and (COD)Pd(CH_3)Cl (71 mg, 0.27 mmol, 1.0 equiv) were dissolved in CH_2Cl_2 (5 mL), and the mixture was stirred for 16 h. Then, it was concentrated in vacuo to approximately 0.5 mL, after which 3 mL of Et_2O was added under vigorous stirring. The white precipitate was filtrated off and washed with Et_2O. Drying in vacuo yielded the product as a white solid (115 mg, 0.22 mmol, 81%). ^{1}H NMR δ (500 MHz, $CDCl_3$) ppm: 9.20 (dd, J = 4.5, 2.0 Hz, 1H, py-H6), 7.62 (dt, J = 7.5, 2.0 Hz, 1H, py-H4), 7.27−7.25 (m, 1H, py-H5), 7.12 (d, J = 7.5 Hz, 1H, py-H3), 6.82 (d, J = 3.0 Hz, 4H, mes-H3), 3.56−3.47 (m, 2H, py-C*H*$_2$), 2.54−2.49 (m, 2H, P−C*H*$_2$), 2.44 (s, 12H, mes-2-C*H*$_3$), 2.24 (s, 6H, mes-4-C*H*$_3$), 0.53 (d, J = 4.5 Hz, 3H, Pd-C*H*$_3$). ^{13}C{^{1}H} NMR δ (75 MHz, $CDCl_3$) ppm: 159.7 (s, py-C2), 152.4 (s, py-C6), 141.4 (d, J = 8.6 Hz, mes-C2), 139.9 (s, mes-C4), 138.4 (s, CH), 131.1 d, J = 7.3 Hz, mes-C3), 129.9 (d, J = 46.4 Hz, mes-C1), 123.9 (s, CH), 123.3 (s, CH), 37.6 (d, J = 5.2 Hz, py-*C*H$_2$), 30.4 (d, J = 31.7 Hz, P-*C*H$_2$), 25.2 (d, J = 7.3 Hz, mes-2-*C*H$_3$), 21.0 (s, mes-4-*C*H$_3$), 1.1 (s, Pd-*C*H$_3$). ^{31}P{^{1}H} NMR δ (121 MHz, $CDCl_3$) ppm: 14.4. Anal. Calcd for $C_{26}H_{33}ClNPPd$: C, 58.66; H, 6.25; N, 2.63. Found: C, 58.60; H, 6.35; N, 2.57. HRMS (FAB) *m*/*z*: calcd for $C_{26}H_{33}NPPd$ [M − Cl]$^+$ 496.1396; found 496.1400.

2-[2-(Di-2-tolylphosphino)ethyl]pyridine Methylpalladium(acetonitrile) Tetrakis[3,5-bis(trifluoromethyl)phenyl]borate (6a). To a mixture of 2-[2-(di-2-tolylphosphino)ethyl]pyridine methylpalladium chloride (**5a**) (148 mg, 275 mmol, 1.0 equiv) and sodium tetrakis[(3,5-trifluoromethyl)phenyl]borate (NaBAr′$_4$) (275 mg, 0.311 mmol, 1.0 equiv) were added CH_3CN (2 mL) and CH_2Cl_2 (10 mL), and the mixture was stirred for 16 h. It was cannula filtrated, evaporated to dryness, and co-evaporated with 5 mL of pentane to yield the product as a white solid (392 mg, 0.291 mmol, 94%). ^{1}H NMR δ (500 MHz, CD_2Cl_2, 25 °C) ppm: 8.58 (bs, 1H, py-H6), 7.80−7.73 (m, 9H, py-H4 + Ar′-H2), 7.68−7.58 (bs, 2H, tol-H6), 7.58 (s, 4H, Ar′-H4), 7.47−7.42 (m, 2H, tol-H4), 7.38−7.29 (m, 4H, py-H3 + -H5 + tol-H5), 7.26−7.20 (m, 2H, tol-H3), 3.50−3.40 (m, 2H, py-C*H*$_2$), 2.58−2.42 (m, 8H, P-C*H*$_2$ + tol-C*H*$_3$), 2.29 (s, 3H, NCC*H*$_3$), 0.26 (s, 3H, Pd-C*H*$_3$). ^{1}H NMR δ (500 MHz, $Cl_2DCCDCl_2$, 80 °C) ppm: 8.63−8.57 (m, 1H, py-H6), 7.78−7.74 (m, 8H, Ar′-H2), 7.72 (t, J = 7.6 Hz, py-H4), 7.60 (dd, J = 14.4, 7.6 Hz, 2H, tol-H6), 7.57 (s, 4H, Ar′-H4), 7.48−7.44 (m, 2H, tol-H4), 7.37−7.33 (m, 2H, tol-H5), 7.29−7.22 (m, 4H, py-H3 + -H5 + tol-H3), 3.44−3.36 (m, 2H, py-C*H*$_2$), 2.55−2.47 (m, 2H, P-C*H*$_2$), 2.48 (s, 3H, tol-C*H*$_3$), 2.24 (s, 3H, NCC*H*$_3$), 0.39 (s, 3H, Pd-C*H*$_3$). ^{13}C{^{1}H} NMR δ (125 MHz, CD_2Cl_2, 25 °C) ppm: 162.4 (q, J = 49.8 Hz, Ar′-C1), 159.9 (s, py-C2), 150.6 (s, py-C6), 141.4 (d, J = 6.3 Hz, tol-C2), 140.2 (s, CH), 135.5 (bs, Ar′-C2), 132.9 (d, J = 8.0 Hz, CH), 132.5 (s, CH), 129.5 (quartet of multiplets, J = 31.6 Hz, Ar′-C3), 128.0 (d, J = 57.3 Hz, tol-C1), 126.7 (d, J = 12.7 Hz, CH), 126.1 (bs, CH), 125.2 (q, J = 272.4, *C*F$_3$), 124.4 (bs, CH), 119.7 (s, N*C*CH$_3$), 118.1 (m, Ar′-C4), 36.9 (s, Py-*C*H$_2$), 25.6 (d, J = 30.3 Hz, P-*C*H$_2$), 23.6 (d, J = 6.3 Hz, tol-*C*H$_3$), 3.2 (s, Pd-*C*H$_3$), 0.7 (s, NC*C*H$_3$). ^{31}P{^{1}H} NMR δ (121 MHz, CD_2Cl_2) ppm: 42.7. ^{19}F{^{1}H} NMR δ (282 MHz, CD_2Cl_2) ppm: −63.0. Anal. Calcd for $C_{56}H_{40}BF_{24}N_2PPd$: C, 50.00; H, 3.00; N, 2.08. Found: C, 49.94; H, 3.06; N, 2.10. HRMS (FAB) *m*/*z*: calcd for $C_{22}H_{25}NPPd$ [M − BAr′$_4$ − CH_3CN]$^+$ 440.0768; found 440.0765. MS (FD) *m*/*z*: 481 [M − BAr′$_4$]$^+$.

2-[2-(Di-2-anisylphosphino)ethyl]pyridine Methylpalladium-(acetonitrile) Tetrakis[3,5-bis(trifluoromethyl)phenyl]borate (6b). To a mixture of 2-[2-(di-2-anisylphosphino)ethyl]pyridine methylpalladium chloride (**5b**) (323 mg, 0.64 mmol, 1.0 equiv) and sodium tetrakis[(3,5-trifluoromethyl)phenyl]borate (NaBAr′$_4$) (563 mg, 0.64 mmol, 1.0 equiv) were added CH_3CN (2 mL) and CH_2Cl_2 (20 mL), and the mixture was stirred for 16 h. It was cannula filtrated, evaporated to dryness, and co-evaporated with 5 mL of hexanes to yield the product as a white solid (762 mg, 0.55 mmol, 87%). ^{1}H NMR δ (500 MHz, CD_2Cl_2, 25 °C) ppm: 8.58 (d, J = 4.9 Hz, 1H, py-H6), 7.79−7.73 (m, 9H, py-H4 + Ar′-H2), 7.58 (s, 4H, Ar′-H4), 7.56−7.51 (m, 2H, anis-H4), 7.54−7.46 (bs, 2H, anis-H6), 7.33 (d, J = 7.8 Hz, 1H, py-H3), 7.32−7.28 (m, 1H, py-H5), 7.04−6.97 (m, 4H, anis-H3 + -H5), 3.85 (s, 3H, anis-C*H*$_3$), 3.46−3.39 (m, 2H, py-C*H*$_2$), 2.46−2.40 (m, 2H, P-C*H*$_2$), 2.29 (s, 3H, NCC*H*$_3$), 0.15 (d, J = 4.2 Hz, 3H, Pd-C*H*$_3$). ^{1}H NMR δ (500 MHz, $Cl_2DCCDCl_2$, 80 °C) ppm: 8.61−8.55 (m, 1H, py-H6), 7.78−7.74 (m, 8H, Ar′-H2), 7.73 (dt, J = 7.7, 1.5 Hz, 1H, py-H4), 7.57 (s, 4H, Ar′-H4), 7.56−7.51 (m, 2H, anis-H4), 7.49 (dd, J = 14.8, 7.4 Hz, 2H, anis-H6), 7.29 (d, J = 7.7 Hz, 1H, py-H3), 7.27−7.23 (m, 1H, py-H5), 7.04−6.99 (m, 4H, anis-H3 + -H5), 3.84 (s, 6H, anis-C*H*$_3$), 3.43−3.34 (m, 2H, py-C*H*$_2$), 2.48−2.43

(m, 2H, P-CH_2), 2.24 (s, 3H, NCCH_3), 0.27 (s, 3H, Pd-CH_3). $^{13}C\{^1H\}$ NMR δ (125 MHz, CD_2Cl_2, 25 °C) ppm: 162.4 (q, J = 49.8 Hz, Ar′-C1), 161.5 (s, anis-C2), 160.6 (s, py-C2), 150.7 (s, py-C6), 139.9 (s, CH), 137.0 (s, CH), 135.5 (bs, Ar′-C2), 134.3 (s, CH), 129.5 (quartet of multiplets, J = 31.6 Hz, Ar′-C3), 125.9 (s, CH), 125.2 (q, J = 272.4, *C*F_3), 123.9 (s, CH), 121.3 (d, J = 12.7 Hz, CH), 119.6 (s, N*C*CH_3), 118.1 (m, Ar′-C4), 117.3 (d, J = 56.4 Hz, anis-C1), 111.9 (d, J = 4.6 Hz, CH), 56.1 (s, anis-CH_3), 36.7 (d, J = 4.6 Hz, py-*C*H_2), 25.5 (d, J = 37.1 Hz, P-*C*H_2), 3.3 (s, NC*C*H_3), −1.0 (s, Pd-*C*H_3). $^{31}P\{^1H\}$ NMR δ (121 MHz, CD_2Cl_2) ppm: 39.7. $^{19}F\{^1H\}$ NMR δ (282 MHz, CD_2Cl_2) ppm: −63.0. Anal. Calcd for $C_{56}H_{40}BF_{24}N_2O_2PPd$: C, 48.84; H, 2.93; N, 2.03. Found: C, 48.90; H, 3.01; N, 2.05. HRMS (FAB) *m*/*z*: calcd for $C_{22}H_{25}O_2NPPd$ [M − BAr′$_4$ − CH_3CN]$^+$ 472.0667; found 472.0664. MS (FD) *m*/*z*: 513 [M − BAr′$_4$]$^+$.

2-[2-(Dimesitylphosphino)ethyl]pyridine Methylpalladium(acetonitrile) Tetrakis[3,5-bis(trifluoromethyl)phenyl]borate (6c). To a mixture of 2-[2-(dimesitylphosphino)ethyl]pyridine methylpalladium chloride (**5c**) (161 mg, 0.302 mmol, 1.0 equiv) and sodium tetrakis[(3,5-trifluoromethyl)phenyl]borate (NaBAr′$_4$) (268 mg, 0.302 mmol, 1.0 equiv) were added CH_3CN (1 mL) and CH_2Cl_2 (10 mL), and the mixture was stirred for 16 h. It was cannula filtrated, evaporated to dryness, and co-evaporated with hexanes and pentane (5 mL each) to yield the product as a white solid (353 mg, 0.252 mmol, 83%). ^1H NMR δ (500 MHz, CD_2Cl_2) ppm: 8.61 (d, J = 5.4 Hz, 1H, py-H6), 7.78−7.73 (m, 9H, py-H4 + Ar′-H2), 7.59 (s, 4H, Ar′−H4), 7.37−7.33 (m, 1H, py-H5), 7.30 (d, J = 7.6 Hz, py-H3), 6.91 (d, J = 3.4 Hz, 4H, mes-H3), 3.51−3.45 (m, 2H, py-CH_2), 2.57−2.54 (m, 2H, P-CH_2), 2.42 (s, 12H, mes-2-CH_3), 2.26 (s, 6H, mes-4-CH_3), 2.22 (s, 3H, NCCH_3), 0.39 (d, J = 3.4 Hz, 3H, Pd-CH_3). $^{13}C\{^1H\}$ NMR δ (125 MHz, CD_2Cl_2) ppm: 162.4 (q, J = 49.8 Hz, Ar′-C1), 160.6 (s, py-C2), 150.5 (s, py-C6), 141.6 (s, mes-C2), 141.5 (s, mes-C4), 140.29 S, CH), 135.5 (bs, Ar′-C2), 131.8 (d, J = 8.9 Hz, mes-C3), 129.5 (quartet of multiplets, J = 31.6 Hz, Ar′-C3), 128.0 (d, J = 42.5 Hz, mes-C1), 125.8 (s, CH), 125.2 (q, J = 272.4, *C*F_3), 124.4 (s, CH), 120.1 (s, N*C*CH_3), 118.1 (m, Ar′-C4), 37.9 (d, J = 4.4 Hz, py-*C*H_2), 30.8 (d, J = 34.6 Hz, P-*C*H_2), 25.2 (d, J = 8.2 Hz, mes-2-CH_3), 21.0 (s, mes-4-*C*H_3), 3.4 (s, NC*C*H_3), 2.1 (s, Pd-*C*H_3). $^{31}P\{^1H\}$ NMR δ (121 MHz, CD_2Cl_2) ppm: 14.7. $^{19}F\{^1H\}$ NMR δ (282 MHz, CD_2Cl_2) ppm: −63.0. HRMS (FAB) *m*/*z*: calcd for $C_{26}H_{33}NPPd$ [M − BAr′$_4$ − CH_3CN]$^+$ 496.1396; found 496.1395. MS (FD) *m*/*z*: 537 [M − BAr′$_4$]$^+$.

General Procedure for the Nickel-Catalyzed Oligomerization. The autoclave was heated to 140 °C under vacuum for 1 h and cooled under a dinitrogen atmosphere. A solution or suspension of the catalyst precursor (10 μmol) in toluene (18.5 mL) was introduced in the reaction chamber, and the autoclave was purged with 10 bar of ethene three times and brought to 10 bar of ethene pressure. After 10 min, the reaction chamber was closed. The injection chamber was vented, and 1.5 mL of MAO in toluene solution (10% w/w, total Al 2.3 mmol) and 5.0 mL of a solution of heptane in toluene (0.20 M, total internal standard 1.0 mmol) were introduced under dinitrogen atmosphere. Then, it was purged with 10 bar of ethene three times and brought to 10 bar of ethene pressure. After 10 min, the injection chamber was closed, the autoclave was disconnected from all lines, and the autoclave was weighed. The autoclave was reconnected, the pressure in the reaction chamber was lowered to ∼8 bar, and the connection between the reaction chamber and the injection chamber was opened, causing the immediate introduction of the MAO and internal standard solution in the reaction chamber. During the run, a constant ethene pressure of 10 bar was applied and the temperature was controlled at 30 °C through the internal cooling spiral against the exotherm of the reaction. After the run, the autoclave was closed and the autoclave was disconnected from all lines and weighed. A sample for gas phase GC analysis was taken, and the autoclave was vented and opened. A 50 mL amount of ice-cold 2 M hydrochloric acid was added to the reaction mixture, and it was stirred vigorously in an ice-bath before samples for liquid phase GC analysis were taken. Ethene consumption was calculated from the increase in weight of the autoclave. Total amount of butenes was calculated from the difference between total ethene consumption and the amount of other oligomers formed.

General Procedure for the Palladium-Catalyzed Oligomerization. The autoclave was charged with the catalyst precursor (100 μmol), closed, brought under dinitrogen atmosphere, and warmed to 30 °C. Then, 25 mL of a solution of heptane in toluene (0.0040 M, total internal standard 0.10 mmol) was introduced, and the autoclave was purged with 10 bar of ethene three times and brought under 10 bar of ethene pressure. After the run, the autoclave was vented and opened. A 50 mL amount of ice-cold 2 M hydrochloric acid was added to the reaction mixture, and it was stirred vigorously in an ice-bath. A sample of the organic phase was cooled to −70 °C and evacuated three times to remove ethene before liquid phase GC analysis was performed.

Acknowledgment. The work described here is part of the research program of the Dutch Polymer Institute (project 106). It was financially supported (M.L., A.L.S.) by the Council for Chemical Sciences of The Netherlands Organization for Scientific Research (CW-NWO). We thank Jurriaan Beckers for gas phase GC measurements and Dr. Bas de Bruin for EPR measurements and discussions.

Supporting Information Available: A CIF file giving crystal data for **4a**, **4c**, **5a**, and **5b** and a file giving variable-temperature ^1H NMR spectra for **5a** and **5b** and general experimental information. This material is available free of charge via the Internet at http://pubs.acs.org.

OM900038U